Lecture: Beta decay

Kenta Hotokezaka

[1]Department of Astrophysical Sciences, Peyton Hall,
Princeton University, Princeton, NJ 08544, USA

August 7, 2018

Physical constants and astrophysical units.

G	6.67384×10^{-8} cm^3 g^{-1}s^{-2}
c	$2.99792458 \times 10^{10}$ cm s^{-1}
h	$6.626070040 \times 10^{-27}$ erg s
$\hbar$	$1.054571628 \times 10^{-27}$ erg s
m_p	$1.6726217 \times 10^{-24}$ g
m_u	$1.6605389 \times 10^{-24}$ g
m_e	$9.10938291 \times 10^{-28}$ g
e	$4.80320425 \times 10^{-10}$ erg$^{1/2}$cm$^{1/2}$
$\alpha = \frac{e^2}{\hbar c}$	$\frac{1}{137.035999139}$
$\sigma_{\rm T} = \frac{8\pi}{3}\left(\frac{e^2}{m_e c^2}\right)^2$	$6.6524574 \times 10^{-25}$ cm^2
$a_{\rm B} = \frac{\hbar}{m_e c \alpha}$	$5.2917721067 \times 10^{-9}$ cm
$k_{\rm B}$	$1.3806488 \times 10^{-16}$ erg K^{-1}
$\sigma_{\rm SB}$	5.6704×10^{-5} erg cm^{-2}s^{-1}K^{-4}
a	7.5657×10^{-15} erg cm^{-3}K^{-4}
$G_F/(\hbar c)^3$	1.1663787×10^{-5} GeV^{-2}
$M_\odot$	1.9884×10^{33} g
$GM_\odot$	$1.32712440018 \times 10^{26}$ cm^{3}s^{-2}
$R_\odot$	6.955×10^{10} cm
$L_\odot$	3.828×10^{33} erg/s
Jy	10^{-23} erg s^{-1}cm^{-2}Hz^{-1}
AU	$1.495978707 \times 10^{13}$ cm
pc	3.08568×10^{18} cm

(1)

1 Introduction

Beta decay is a type of radioactive decay in which an electron (or positron) and a neutrino are emitted. Through this disintegration process, a neutron (proton) is converted to a proton (neutron). One of the famous examples is free neutron decay with a mean lifetime of 881.5 ± 1.5 s (~ 15 min) and an energy release 0.782 ± 0.13 MeV.

Nucleons in a nucleus move with a velocity of $\sim 0.1c$. Given the typical size of nuclei $\sim \mathcal{O}$(fm), the orbiting time scale of a nucleon in a nucleus is $\sim 10^{-22}$ s. In a beta decay time scale, say $\sim 10^4$ s, a nucleon orbits about 10^{26} times (c.f. Earth has been orbiting around the Sun $\sim 5 \cdot 10^{10}$ times). This means that beta-unstable nuclei are extremely stable against the beta decay, and hence, we can consider beta decay separately from other nuclear processes, i.e., we don't have to worry about beta decay of excited nuclei. This long time scale of beta decay simplifies the problem.

Since the energy scale of electrons emitted in beta decay is about electron mass, the electron's (and neutrino's) de Broglie wavelength is about the Compton wavelength:

$$\lambda_c = \frac{h}{m_e c} \approx 2500\,\text{fm}. \tag{2}$$

Therefore, the disintegrated nucleus is practically a point without a physical size for the light particles.

Remarkable features of beta decay are summarized

- the energy scale is about the electron mass,
- the time scale is extremely long,
- half-lives of beta unstable nuclides are distributed in a wide range (many orders of magnitude),
- half-lives increase with decreasing the disintegration energy approximately as $\sim E^{-3} - E^{-5}$.

2 A brief introduction of r-process nucleosynthesis

Nuclear mass formula: The nuclear mass of a nuclide of a mass number of A and an atomic number of Z is given by

$$M(A,Z) = Zm_p + (A-Z)m_n - \frac{E_B(A,Z)}{c^2}, \tag{3}$$

where the last term is empirically given by

$$E_B = a_V A - a_s A^{2/3} - a_C \frac{Z(Z-1)}{A^{1/3}} - a_A \frac{(A-2Z)^2}{A} + \delta(A,Z). \tag{4}$$

Here $\delta(A,Z)$ is the paring energy: δ_0 for Z and $A-Z$, even, 0 for A odd, and $-\delta_0$ for Z and $A-Z$ odd. The constants are empirically determined. The fourth term represents asymmetric energy. One can see that more and more neutron rich nuclei have smaller biding energy and more unstable against beta decay. Note also that there is a limit on the neutron number for a given Z, where nuclei cannot bound any additional neutrons. The line defined by this limit on Z-$(A-Z)$ plane is called the neutron drip line.

R-process is a nucleosynthesis process, where free neutrons are synthesized into nuclei on a timescale much shorter than the time scale of beta decay (the reaction occurs typically on time scales much shorter than 1 s). This is one of a few processes that can astrophysically produce elements beyond the iron peak elements. R-process nucleosynthesis proceeds from a small to large A through a path close to the neutron drip line (figure 2). For instance, neutron merger ejecta are one of the most favored astrophysical sites of r-process because the expanding material is highly neutron rich. Figure 2 shows the abundance distribution of nuclides just after r-process nucleosynthesis in a neutron merger ejecta. Remarkably, almost all nucleons are synthesized into heavy nuclei and they are distributed in a wide range of A. Furthermore, the nuclides' distribution soon after r-process is far away from the valley of stability marked as thick boxes in figure 2. These nuclei with a mass number of $A \lesssim 210$ approach the valley of stability via beta decay. Superheavy nuclei are disintegrated through alpha decay and/or fission. In the following, we discuss about the radioactive heats, which are the standard energy source of kilonovae, generated after r-process nucleosynthesis.

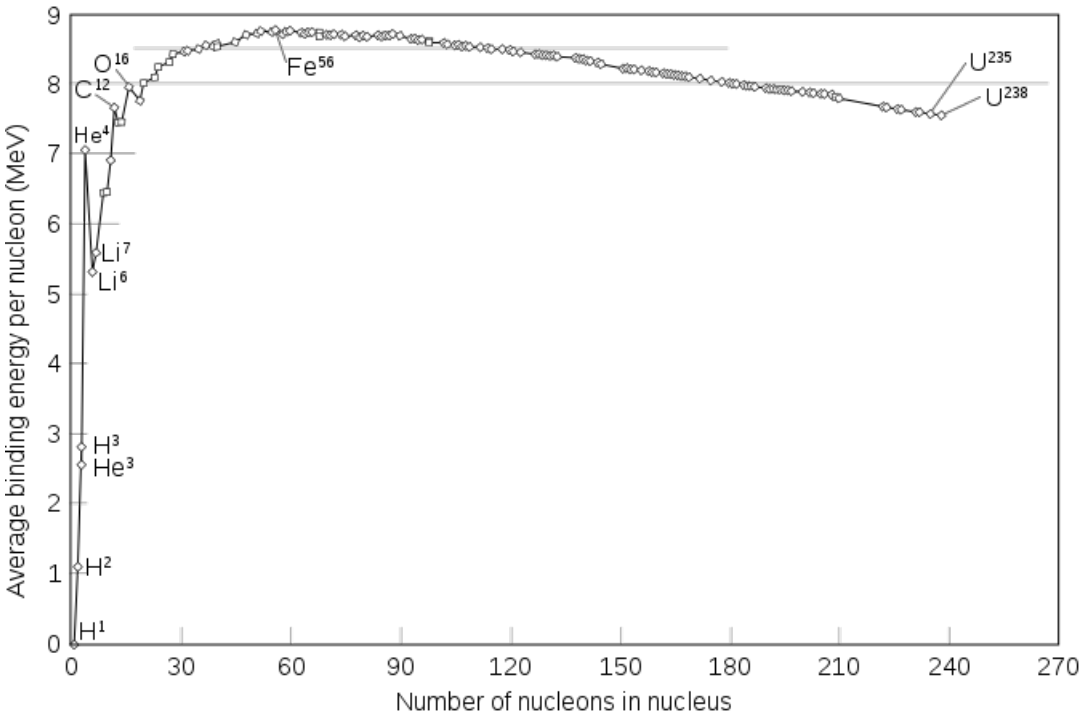

Figure 1: Nuclear binding energy per nucleon.

3 A short summary of beta-decay heating rate

Radioactive nuclei that are far from the stability valley are produced in r-process nucleosynthesis. These nuclei undergo beta decay without changing their mass number. A series of beta decays in each mass number is considered as a decay chain. Because the mean lives of radioactive nuclides typically become longer when approaching the stability valley, the nuclei in a decay chain at given time t stay at some specific nuclide with a mean life $\tau \sim t$. This means that the number of decaying nuclei in a logarithmic time interval is constant, i.e, the decay rate is $\sim N/t$, where N is the total number of nuclei in the chain. Then the beta decay heating rate per nucleus is given by $\dot{q} \sim E(t)/t$, where $E(t)$ is the disintegration energy of the beta decay as a function of the mean life. As we will see later, two important concepts in beta decay theory enable us to determine $E(t)$. First, there are practically four physical constants in the problem, the Fermi's constant G_F, the electron mass m_e, the speed of light c, and the Planck constant $\hbar$. The fundamental timescale of beta decay $t_F \approx 9 \cdot 10^3$ s can be obtained from these physical constants. Second, there is a well known relation between the disintegration energy and mean life as $\tau \propto E^{-5}$. Therefore, the heating rate per nucleus can be roughly estimated as

$$\dot{q}(t) \sim \frac{m_e c^2}{t_F} \left(\frac{t}{t_F} \right)^{-1.2}. \tag{5}$$

This gives a correct order of magnitude and a reasonable estimate of the time dependence of the beta decay heating rate of r-process material. In the following we refine these ideas.

4 Beta decay

Fermi successfully developed a theoretical model which describes the beta disintegration very well. In Fermi's theory, four particles, beta ray, neutrino, neutron, and proton, interact at a single point (Fig. 5) analogous to the photon and charged particle interaction in quantum electromagnetic dynamics.

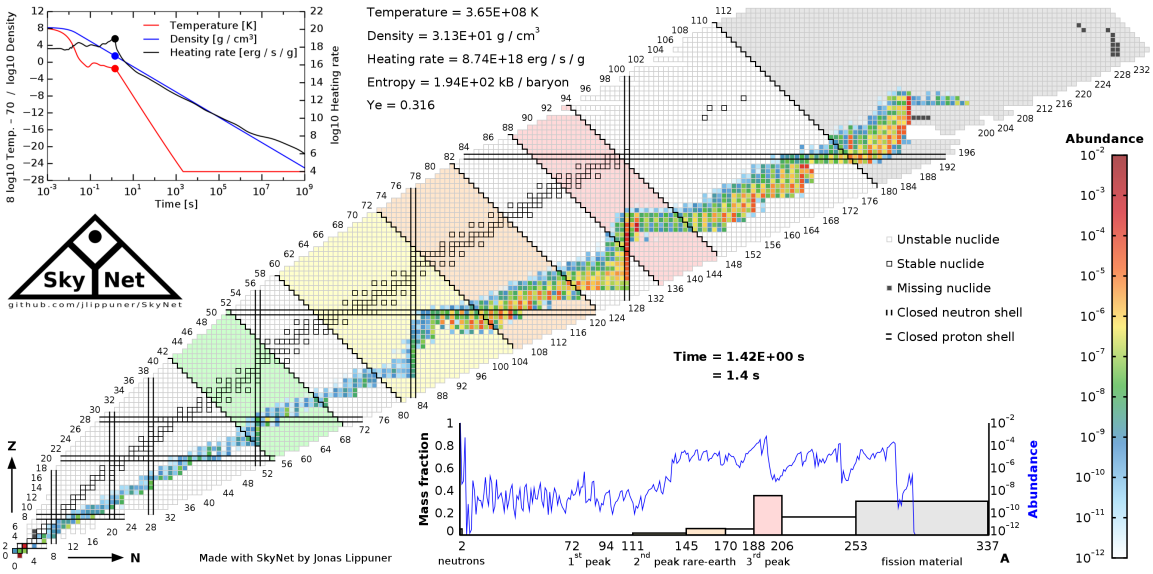

Figure 2: R-process nucleosynthesis simulation of neutron star merger ejecta. The figure is taken from Lippuner and Roberts (2015).

Kinematics: The final state of the disintegration process with a disintegration energy $\bar{E}_0$ radiates an electron of $\vec{p}_e$ and $\bar{E}_e$ including rest mass energy[1], neutrino of $\vec{p}_\nu$ and E_ν. Let us first consider how $\bar{E}_0$ is distributed among the particles. From here and elsewhere we consider the parent nucleus is at the coordinate origin at rest. The maximum recoil energy of the daughter nucleus occurs when all the disintegration energy is transferred to the electron, i.e., $\bar{E}_e = \bar{E}_0$. The momentum of the electron is then

$$\frac{p_e}{m_e c} = \left[\left(\frac{\bar{E}_0}{m_e c^2} \right)^2 - 1 \right]^{1/2}, \tag{6}$$

The recoil momentum must be equal to this value so that we find

$$\frac{E_{\rm rec}}{\bar{E}_0} = \frac{1}{2m_A} p_e^2 = \frac{m_e}{2m_A} \left(\frac{\bar{E}_0}{m_e c^2} - \frac{m_e c^2}{\bar{E}_0} \right). \tag{7}$$

For beta decay, the second factor is less than 30 and the first factor is $< 10^{-4}$. Therefore, the recoil energy of the daughter nucleus is negligible and the available disintegration energy is distributed just to the electron and neutrino:

$$\bar{E}_0 = \bar{E}_e + E_\nu. \tag{8}$$

The same relation hold for kinetic energy as

$$E_0 = E_e + E_\nu, \tag{9}$$

where $E_0 = \bar{E}_0 - m_e c^2$.

Disintegration probability: In beta decay, two particles, electron and neutrino, are created. We start by assuming, as Fermi did, that all possible divisions of energy are equally likely. That says, the disintegration probability is proportional to the *accessible* phase space volume of the two particles. Here the *accessible* means a part of the phase space where the energy conservation $E_0 = E_e + E_\nu$ is satisfied.

Consider that in the final state of a disintegration the electron is contained in the volume element dV_e and has a momentum of magnitude between p_e and $p_e + dp_e$ in a direction within the solid

[1] $\bar{E}$ is energy including the rest mass and $E = \bar{E} - mc^2$ denotes kinetic energy. For neutrino, we just use E_ν as its mass is negligibly small for our problem.

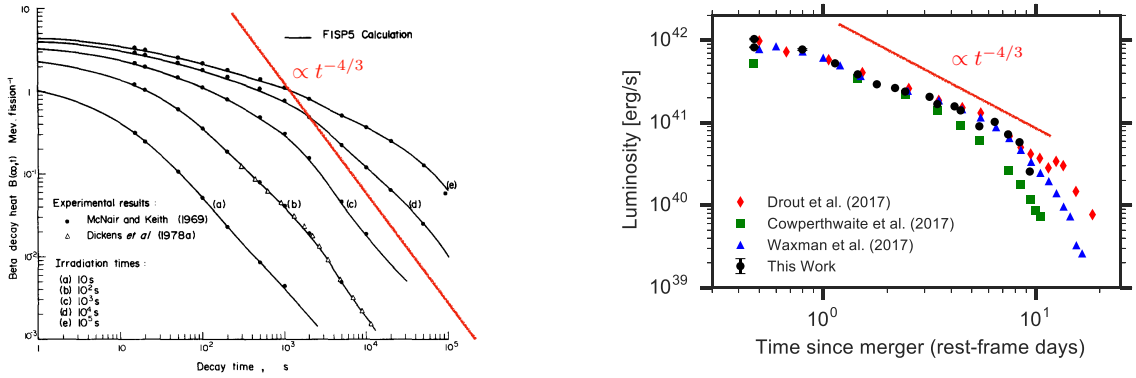

Figure 3: Beta decay heating rate of fission products of ^{238}Pu (*left*, adopted from Tobias, Progress in Nuclear Energy, 5, p1, 1979) and bolometric luminosity of the kilonova GW170817 (*right*, adopted from Arcavi, ApJL, 855, L23, 2018)

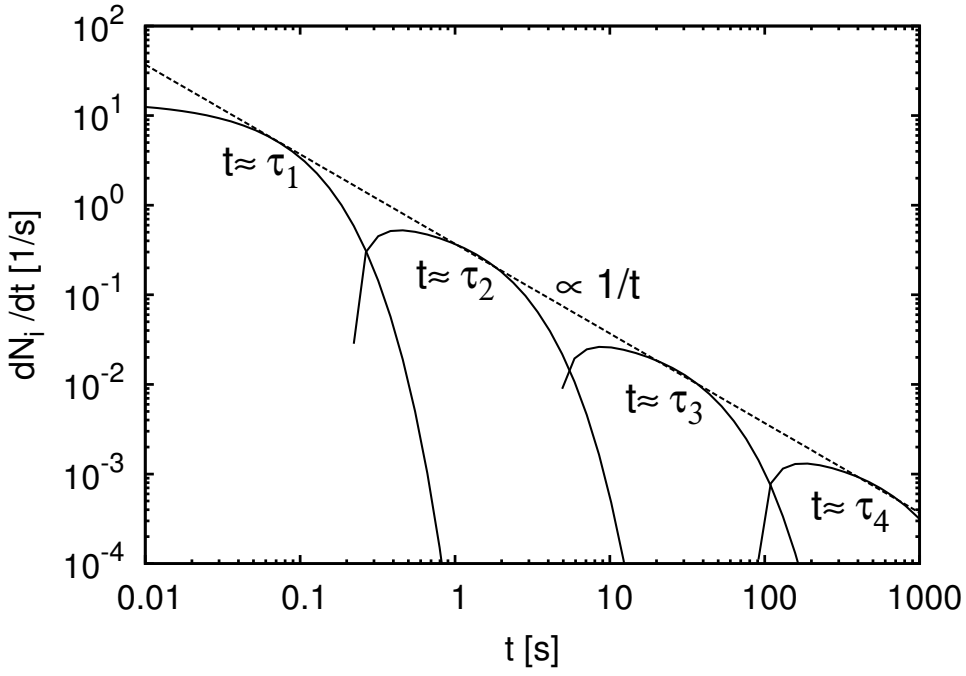

Figure 4: A decay chain normalized by the total number of nuclei in the chain. The dashed line depicts e^{-1}/t, where e is Euler number.

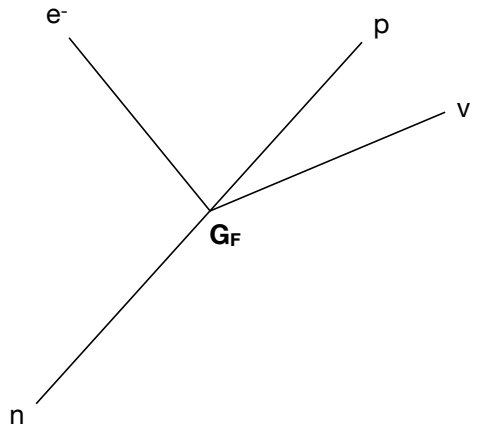

Figure 5: Four Fermi interaction.

angle element $d\Omega_e$. Corresponding statements hold for the neutrino. The volume of this state in phase space is expressed in units of $(2\pi\hbar)^6$, which leads to

$$\text{Phase space vol.} = \frac{1}{(2\pi\hbar)^6} p_e^2 dp_e d\Omega_e dV_e p_\nu^2 dp_\nu d\Omega_\nu dV_\nu. \tag{10}$$

Now we use the energy conservation as

$$dp_\nu = \left(\frac{\partial p_\nu}{\partial E_0}\right)_{p_e} = \frac{dE_0}{c}. \tag{11}$$

Using this, the phase space volume assumes the form of $\rho(E_0)dE_0$, where dE_0 is the density of final states per unit range of total energy:

$$\rho(E_0) = \frac{1}{(2\pi\hbar)^6} \frac{1}{c^3} p_e^2 (E_0 - E_e)^2 dp_e d\Omega_e dV_e d\Omega_\nu dV_\nu. \tag{12}$$

The probability that the beta decay leads to this particular final state is proportional to $\rho(E_0)$.

Since we are not concerned about the location of the particles, we just integrate over dV. Furthermore, we assume no angular correlation between the particles then we have

$$\rho(E_0) = \frac{V^2}{4\pi^4\hbar^6 c^3} p_e^2 (E_0 - E_e)^2 dp_e. \tag{13}$$

The shape of $\rho(E_0)$ is called as the allowed beta spectrum. The momentum distribution of emitted electrons follows equation (13).

A quantum transition from a state to another due to a small perturbation described by H' is proportional to the number of the final states and square of the matrix element of H'. Using Fermi's Golden rule, the beta-disintegration probability of a beta-unstable nucleus per unit time in a unit momentum interval of the electron is written as

$$\frac{dw}{dp_e} dp_e = \frac{2\pi}{\hbar} \left|H'_{fi}\right|^2 \rho(E_0), \tag{14}$$

where H'_{fi} is the matrix element of the interaction Hamiltonian responsible for the beta disintegration.

In Fermi's theory, the four particles interact at a single point with a coupling constant G_F. The matrix element is written as

$$H'_{fi} = G_F \sum_{n=1}^{A} \int (\psi_e^\dagger \mathcal{O}_L \psi_\nu^*)(\psi_f^\dagger \mathcal{O}_{N,n} \psi_i) dV, \tag{15}$$

where ψ_e and ψ_ν are the electron and neutrino wave functions, ψ_i and ψ_f are the nuclear wave functions of the initial and final states. $\mathcal{O}_L$ and $\mathcal{O}_{N,n}$ are operators acting on the light particle's spin, and spin and isospin of the nth nucleon undergoing beta decay.

Let us consider now non-relativistic limit for simplicity. The wave functions of the light particles are

$$\psi_e(\vec{r_e}) = \frac{1}{\sqrt{V}} u_e \exp(i\vec{p} \cdot \vec{r_e}), \tag{16}$$

$$\psi_\nu(\vec{r_\nu}) = \frac{1}{\sqrt{V}} u_\nu \exp(i\vec{q} \cdot \vec{r_\nu}), \tag{17}$$

$$\tag{18}$$

where u_e and u_ν are Pauli spinors, e.g., $u_e^T = (1, 0)$.

$$\psi_e^\dagger \mathcal{O}_L \psi_\nu^* = \frac{1}{V} (u_e^\dagger \mathcal{O}_L u_\nu^*) \exp\left(-i(\vec{p} + \vec{q}) \cdot \vec{r}\right). \tag{19}$$

The wave part can be expanded to an arbitrary direction (Θ, Φ) as

$$\exp(i\vec{k} \cdot \vec{r}) = 4\pi \sum_{l=0}^{\infty} \sum_{l=-m}^{l} i^l j_l(kr) Y_{lm}^*(\Theta, \Phi) Y_{lm}(\theta, \phi), \tag{20}$$

where θ is the angle between $\vec{k}$ and $\vec{r}$, and ϕ is the azimuthal angle. Because the de Broglie wavelengths of the electron and neutrino are much larger than the nuclear size, $(p + q)r$ is so small that the wave function of the light particles is dominated by lower l-modes. When the light particles do not carry off orbital angular momentum with respect to the central nucleus ($l = 0$), the wave function of each light particle at $r = 0$ is just a normalization factor of $V^{-1/2}$ with a Coulomb correction for the electron's wave function, $|\psi_e|_Z^2 / |\psi_e|_{Z=0}^2$. Thus the square of the matrix element can be written as

$$|H'_{fi}|^2 = \frac{G_F^2}{V^2} F(Z, E) |\mathcal{M}_N|^2, \tag{21}$$

where $F(Z, E)$ is the Coulomb correction factor, Z is the proton number of the daughter nucleus, and $\mathcal{M}_N$ is the nuclear matrix element. The transitions described here are *allowed* transition. More specifically, allowed transitions are transitions which satisfy both conditions that the light particles don't carry off orbital angular momentum and the parity of the nucleus does not change via its disintegration. Otherwise the transition is a *forbidden* transition.[2] Because the population of allowed transitions is larger and because of their simplicity, we focus on allowed transitions.

Integrating Eq. (14) over the accessible phase space, the mean-life of a beta-unstable nuclide with the disintegration energy of E_0 is obtained as

$$\frac{1}{\tau} = \frac{|\mathcal{M}_N|^2}{t_F} \int_0^{p(E_0)} dp F(Z, E) p^2 (E - E_0)^2, \tag{22}$$

where the variables in the integral are in units of m_e and c and t_F is the fundamental timescale of beta decay:

$$t_F \equiv \frac{2\pi^3}{G_F^2} \frac{\hbar^7}{m_e^5 c^4} \approx 8610 \text{ s}.$$

[2] We employ Konopinski's classification of beta decay (Konopinski, 1966).

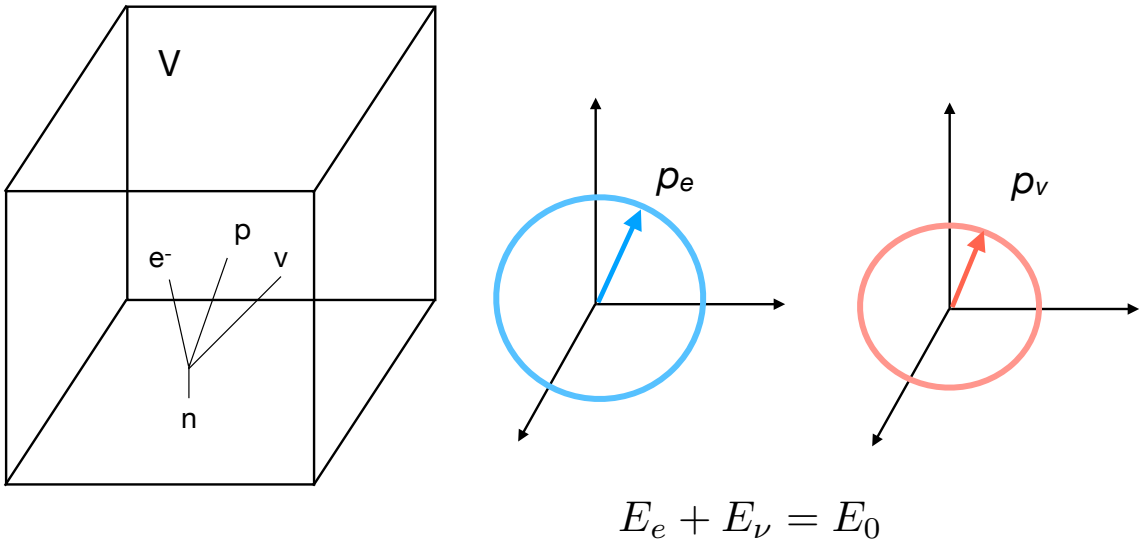

Figure 6: Four Fermi interaction.

Note that, although this fundamental timescale is a characteristic timescale of allowed beta decay, the lifetime of beta unstable nuclides spreads over many orders of magnitude because of the phase space factor of Eq. (22).

The Coulomb correction factor in the matrix element is obtained by evaluating the electron's wave function at the nuclear radius r_n (Fermi, 1934):

$$\begin{aligned} F(Z,E) &\cong \frac{|\psi_e(r_n)|^2_Z}{|\psi_e(r_n)|^2_{Z=0}}, \\ &= \frac{2(1+s)}{[(2s!)^2]}(2p\rho)^{2s-2}e^{\pi\eta}\left|(s-1+i\eta)!\right|^2, \end{aligned} \tag{23}$$

where $\eta = Zq_e^2/\hbar v$, v is the velocity of the electron, $\rho = r_n/(\hbar/m_e c)$, $s = (1-(Z\alpha)^2)^{1/2}$, q_e is the electron charge, and $\alpha \approx 1/137$ is the fine-structure constant. For $E > 1$, the Coulomb correction factor slowly increases with E as $F(Z,E) \propto E^{2s-2}$.

A simple form of the Coulomb correction factor is obtained in the non-relativistic limit of Eq. (23), $\eta \gg 1$ and $(Z\alpha)^2 \to 0$:

$$F_N(Z,E) = \frac{2\pi\eta}{1-\exp(-2\pi\eta)}. \tag{24}$$

The Coulomb correction factor is unity for $\eta \ll 1$ and approaches $2\pi\eta$ for $\eta \gg 1$. This enhances the transition probability at lower energies. At these energies the electron is pulled by the nucleus due to the Coulomb force and the amplitude of the electron's wave function is larger near the nucleus. As a result, the lifetime of beta unstable nuclei becomes shorter than the one estimated without

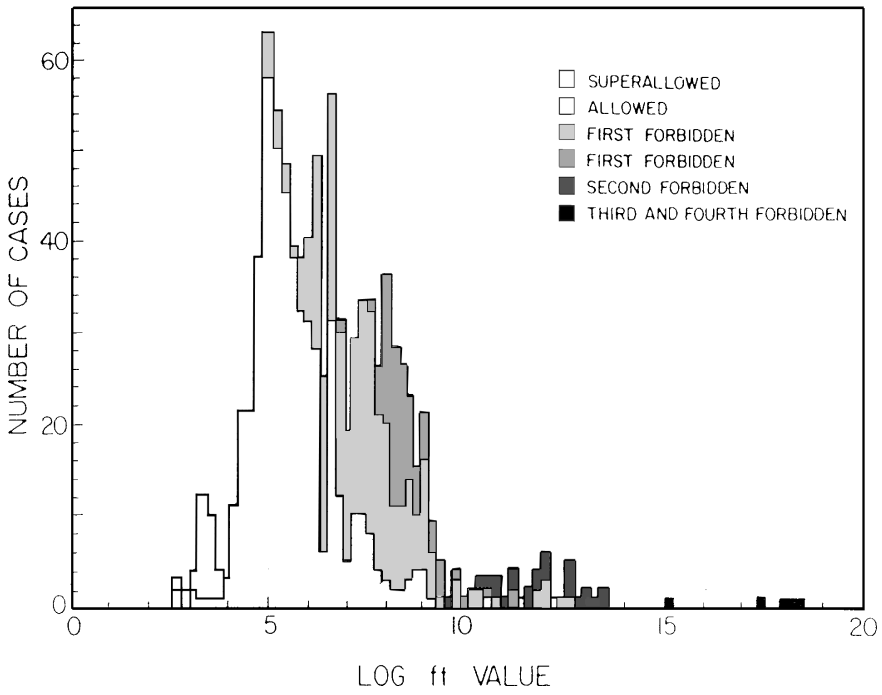

Figure 7: Comparative half-lives. (Adapted from G. E. Gleit et al., Nucl. Data Sheets 5 1963 set 5.)

the Coulomb correction and the dependence of the lifetime on E_0 is weakened. Note that one can also obtain an identical form to Eq. (24) by solving the Schrödinger equation and evaluating the electron's wave function at $r = 0$.

As the integral in Eq. (22) is easily calculated for given E_0 and Z, comparative half-lives $ft_{1/2}$ are often used for comparison with the experimental data:

$$ft_{1/2} \equiv \frac{\ln 2}{|\mathcal{M}_N|^2} t_F. \tag{25}$$

Although $\mathcal{M}_N$ of each beta transition cannot be calculated within Fermi's theory, $\mathcal{M}_N$ can be determined from the measurements of the lifetime and the electron's spectrum. It is sufficient for our purpose to know the statistical distribution of this quantity. For allowed transitions, the distribution of $ft_{1/2}$ is known to have a peak around 10^5 s corresponding to $|\mathcal{M}_N|^2 \sim 0.05$ (see figure 7), which we take as a reference value in this paper.[3]

Now we evaluate the integral of

$$f(E_0, Z) = \int_0^{p(E_0)} dp F(Z, E) p^2 (E - E_0)^2, \tag{26}$$

$$= \int_0^{E_0} dE F(Z, E)(E + 1)\sqrt{(E + 1)^2 - 1}(E - E_0)^2. \tag{27}$$

One can show that f attains simple forms in the following three regimes:

(i) relativistic regime ($E_0 \gg m_e c^2$ and $Z\alpha/\beta \ll 1$): In this regime, we can neglect electron mass

[3]For neutron and mirror nuclides such as ^{3}H, the comparative half-lives are $\sim 10^3$ s corresponding to $|\mathcal{M}_N|^2 \sim 1$. Such transitions are called as *superallowed* transitions. These transitions are, however, absent in r-process material.

and the Coulomb correction in the beta spectrum.

$$
\begin{aligned}
f(E_0, Z) &= \int_0^{E_0} dE F(Z,E)(E+1)\sqrt{(E+1)^2-1}(E-E_0)^2, && (28)\\
&\approx \int_0^{E_0} dE E^2 (E-E_0)^2, && (29)\\
&= \frac{1}{30} E_0^5. && (30)
\end{aligned}
$$

(ii) Non-relativistic regime ($E_0 \ll m_e c^2$ and $Z\alpha/\beta \ll 1$):

$$
\begin{aligned}
f(E_0, Z) &= \int_0^{E_0} dE F(Z,E)(E+1)\sqrt{(E+1)^2-1}(E-E_0)^2, && (31)\\
&\approx \sqrt{2}\int_0^{E_0} dE E^{1/2} (E-E_0)^2, && (32)
\end{aligned}
$$

where we used an approximation $E_0 \ll 1$. We find

$$
f(E_0, Z) \approx \frac{16\sqrt{2}}{105} E_0^{7/2}. \quad (33)
$$

(ii) Non-relativistic Coulomb regime ($E_0 \ll m_e c^2$ and $Z\alpha/\beta \gg 1$):

$$
\begin{aligned}
f(E_0, Z) &= \int_0^{E_0} dE F(Z,E)(E+1)\sqrt{(E+1)^2-1}(E-E_0)^2, && (34)\\
&\approx \sqrt{2}\int_0^{E_0} dE \frac{2\pi Z\alpha}{\beta} E^{1/2} (E-E_0)^2. && (35)\\
& && (36)
\end{aligned}
$$

Using $E = \beta^2/2$, we find

$$
\begin{aligned}
f(E_0, Z) &\approx 2\pi Z\alpha \int_0^{E_0} dE (E-E_0)^2. && (37)\\
&= \frac{2\pi Z\alpha}{3} E_0^3. && (38)
\end{aligned}
$$

$$
f(Z, E_0) = \begin{cases} \frac{1}{30} E_0^5 & (\text{relativistic}: \ E_0 > 1), \\ \frac{16\sqrt{2}}{105} E_0^{7/2} & (\text{non relativistic}: \\ & \quad E_c < E_0 < 1), \\ \frac{2\pi Z\alpha}{3} E_0^3 & (\text{non relativistic Coulomb}: \\ & \quad E_0 < \min(E_c, 1)), \end{cases} \quad (39)
$$

where $E_c = (2\pi Z\alpha)^2/2$. The non-relativistic regime exists only for $Z \lesssim 30$, and thus, there is no such a regime in r-process material. In previous a work Colgate & White (1966) applied only the relativistic regime $\tau \propto E^{-5}$. However, as we will see later, the mean-lives of the nuclei are rather proportional to E^{-4} or E^{-3} on the relevant timescale of macronovae, i.e., a few days.

In the context of macronovae, we are interested in the relation between the lifetime and the mean electron's energy since the neutrinos don't contribute to the heat deposition in the merger ejecta. The fraction of energy of the electrons to the total energy is:

$$
\begin{aligned}
\epsilon_e &\equiv \frac{\langle E_e \rangle}{E_0}, && (40)\\
&= \frac{1}{\epsilon_0} \frac{\int_0^{p_0} E_e F(Z,p) p^2 (E_0 - E)^2 dp}{\int_0^{p_0} F(Z,p) p^2 (E_0 - E)^2 dp}.
\end{aligned}
$$

In the three regimes discussed earlier ϵ_e satisfies:

$$\epsilon_e = \begin{cases} 1/2 & (\text{relativistic} : E_0 > 1), \\ 1/3 & (\text{non relativistic} : (E_c < E_0 < 1), \\ 1/4 & (\text{nr Coulomb} : E_0 < E_c), \end{cases} \tag{41}$$

where we assumed $E_c < 1$.

5 The heating rate: the ideal-chains approximation

Neutron-rich nuclei produced via the r-process undergo beta decay towards the beta-stable valley without changing their mass number. A series of beta decays of nuclei in each mass number can be considered as a decay chain. Here we consider ideal-chains of radioactive nuclei with a series of mean lives ($\tau_1 < \tau_2 < \tau_3 < ...$), in which each chain conserves the total number of nuclei throughout the decay process and sufficiently many chains exist. Within this approximation, the number of decaying nuclei in a logarithmic time interval is constant and the beta decays at a given time t are dominated by nuclides with mean-lives of $\tau \sim t$ (see Fig. 4). This is, of course, valid for $t > \tau_1$, where τ_1 is the mean life of the first nuclide in a decay chain. The heating rate per unit mass is then

$$\dot{Q}(t) = -\sum_i \frac{E_{e,i}}{\langle A \rangle m_u} \frac{dN_i}{dt} \approx \frac{e^{-1}}{\langle A \rangle m_u} \frac{\langle E_e(t) \rangle}{t}, \tag{42}$$

where $\langle A \rangle$ is the mean mass number of the r-process material, and m_u is the atomic mass unit. Note that e is the Euler number, which arises from the fact that the decay rate of each nuclide is proportional to $e^{-t/\tau}$. One can obtain $\dot{Q}$ by using Eq. (22) and (11).

In the relativistic and non-relativistic Coulomb regimes, we can derive simple explicit forms of Eq. (42). As the lifetime of beta-unstable nuclides monotonically increases with decreasing E_0, the relativistic regime is valid at early times and the non-relativistic Coulomb regime is valid at late times. More specifically, the relativistic regime is valid until $t_{\rm R} \approx 10^3\,{\rm s}\,(0.05/|\mathcal{M}_N|^2)$ and the non-relativistic Coulomb regime is valid after $t_{\rm NC} \approx 10^6\,{\rm s}\,(0.05/|\mathcal{M}_N|^2)$. Using Eqs. (39) and (41), we obtain the heating rate in these regimes:

$$\dot{Q}(t) \approx \begin{cases} 1.2 \cdot 10^{10}\ \frac{\rm erg}{\rm s \cdot g}\ t_{\rm day}^{-\frac{6}{5}} \\ \qquad \times \langle A \rangle_{200}^{-1} \left(\frac{|\mathcal{M}_N|^2}{0.05} \right)^{-\frac{1}{5}} \qquad (t \lesssim t_{\rm R}), \\ 0.3 \cdot 10^{10}\ \frac{\rm erg}{\rm s \cdot g}\ t_{\rm day}^{-\frac{4}{3}} \\ \qquad \times \langle Z \rangle_{70}^{-\frac{1}{3}} \langle A \rangle_{200}^{-1} \left(\frac{|\mathcal{M}_N|^2}{0.05} \right)^{-\frac{1}{3}} \quad (t \gtrsim t_{\rm NC}), \end{cases} \tag{43}$$

where $t_{\rm day}$ is time in units of a day, $\langle A \rangle_{200}$ is the mean mass number normalized by 200, and $\langle Z \rangle_{70}$ is the mean proton number normalized by 70. Note that the overall magnitude of the heating rate is determined by the mean values of the nuclear quantities, A, Z, and $\mathcal{M}_N$. These values should be constant within an order of magnitude, and thus, the magnitude of the heating rate does not depend significantly on the details of the abundance pattern of the r-process nuclei. Furthermore, we emphasize that the formula of Eq. (43) is independent of the distribution of the nuclear decay energy.

Figure 8 depicts the heating rate obtained from Eq. (42) and the one derived using a nuclear database (Hotokezaka et al. 2016; see also similar heating rates in Metzger et al. 2010; Goriely et al. 2011; Roberts et al. 2011; Korobkin et al. 2012; Wanajo et al. 2014; Lippuner & Roberts 2015). We find that the heating rate based on the simple analytic formula reproduces the one based on the database remarkably well. In order to see more details, the right panel of Fig. 8 shows the heating rates normalized to the values obtained for the relativistic regime (Eq. 43). The normalized analytic heating rate (blue solid line) is flat at early times and it approaches the non-relativistic Coulomb regime (magenta dotted line) at late times.

It is worthy noting that the formula with the non-relativistic Coulomb limit reproduces the full heating rate after 10^3 s, even though it should be valid only after $\sim 10^6$ s. This can be understood

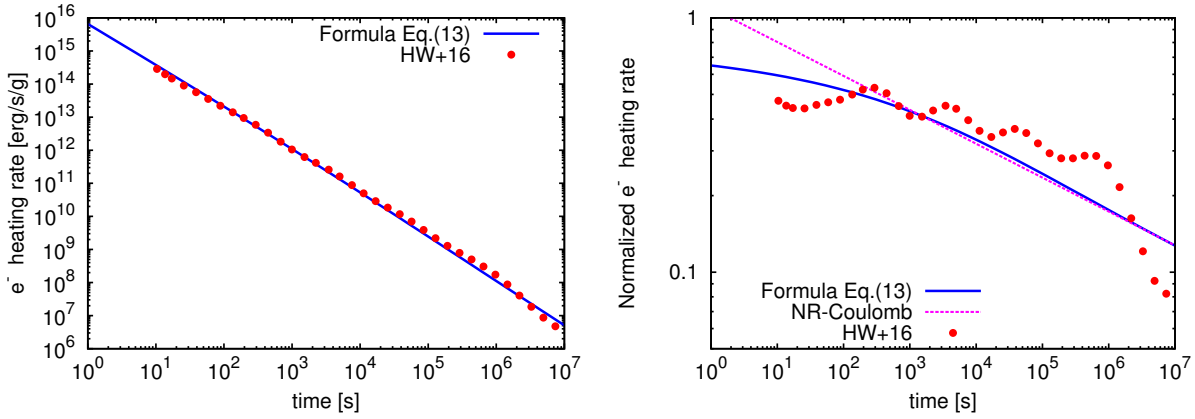

Figure 8: The heating rate of the ideal chains of allowed beta decay by electrons. Left panel: the specific heating rate derived by Eq. (42). Right panel: the heating rate normalized by the relativistic regime of Eq. (43). Also shown in both panels is the electron heating rate taken from Hotokezaka et al. 2016, where the heating rate is obtained by using Evaluated Nuclear Data File. Here we adopt $|\mathcal{M}_N|^2 = 0.05$, $\langle A \rangle = 200$, and $\langle Z \rangle = 50$ for the analytic model.

as follows. The mean life is approximately proportional to E_0^{-4} between the relativistic and the non-relativistic regimes, and thus, the energy generation rate evolves as $E_0/t \propto t^{-\frac{5}{4}}$. In addition, in this stage, ϵ_e changes from 1/2 to 1/4, which approximately corresponds to $\epsilon_e \propto t^{-\frac{1}{9}}$. As a result, the electron heating rate is $\propto t^{-1.35}$, which is quite similar to the one in the non-relativistic Coulomb regime.

5.1 Free Neutron Lifetime

The lifetime of neutron $\tau_n = 880.3 \pm 1.1$ s (Particle Data Group 2014) is described as

$$\frac{1}{\tau_n} = \frac{2\pi}{\hbar}\frac{G_s^2 + 3G_t^2}{4\pi^4\hbar^6c^3}\int_0^{p_{e,0}} F(Z,E)p_e^2(E_0 - E_e)^2 dp_e, \quad (44)$$

$$= \frac{V_{ud}^2 + 3C_A^2}{t_F} f(\tilde{E}_0), \quad (45)$$

$$= \frac{V_{ud}^2(1+3\lambda^2)}{t_F} f(\tilde{E}_0), \quad (46)$$

where

$$t_F \equiv \frac{2\pi^3 m_e^2 c^4}{G_F^2}\left(\frac{\hbar}{m_e c}\right)^6\left(\frac{\hbar}{m_e c^2}\right) \quad (47)$$

$$= 8611.3 \text{ s}, \quad (48)$$

V_{ud} is the first element of the Cabbibo-Kobayashi-Maskawa matrix, $G_F/(\hbar c)^3 = 1.1663787 \times 10^{-5}$ GeV^{-2} determined from muon decay. $V_{ud} = 0.97425$ (22) is measured by ft-value of superalllowed $0^+ \to 0^+$ beta decay systems and $\lambda = -1.2723 \pm 0.0023$ is measured by neutron decay.

5.2 Coulomb wave function

In the non-relativistic limit, the Coulomb correction to the beta decay lifetime can be obtained from an exact solution of the Schrodinger equation. The equation for an electron in a Coulomb potential is

$$-\frac{\hbar^2}{2m_e}\nabla^2\psi - \frac{Ze^2}{r}\psi = E\psi, \quad (49)$$

$$\frac{d^2\chi}{dR^2} + \left(1 - \frac{l(l+1)}{R^2} + \frac{2\eta}{R}\right)\chi = 0, \quad (50)$$

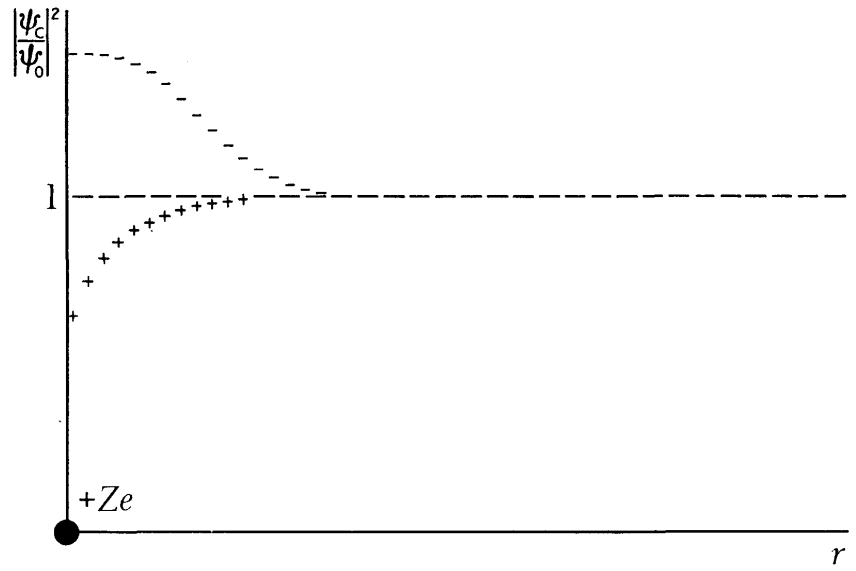

Figure 9: Coulomb correction factor. Adopted from Konopinski (1966).

where $\psi = \chi\Phi/r$, $\nabla_\perp^2\Phi = -l(l+1)/r^2$, $R = kr$, and

$$k^2 = \frac{2m_eE}{\hbar^2} \quad \eta = \frac{m_eZe^2}{\hbar^2 k}. \tag{51}$$

We also used $m_em_N/(m_e+m_N) \approx m_e$. Equation (50) is known as the Coulomb differential equation (Abramowitz and Stegun):

$$\frac{d^2w}{d\rho^2} + \left(1 - \frac{2\eta}{\rho} - \frac{L(L+1)}{\rho^2}\right) w = 0, \tag{52}$$

where $\rho > 0$, $-\infty < \eta < \infty$, and L is a non-negative integer. The general solution is given by

$$w = C_1F_L(\eta,\rho) + C_2G_L(\eta,\rho), \tag{53}$$

where $F_L(\eta,\rho)$ is the regular Coulomb wave function and $G_L(\eta,\rho)$ is the irregular Coulomb wave function. Since the latter diverges at $\rho \sim 0$, we are interested in F_L, which is given by

$$F_L(\eta,\rho) = C_L(\eta)\rho^{L+1}e^{-i\rho}M(L+1-i\eta, 2L+2, 2i\rho), \tag{54}$$

where $M(L+1-i\eta, 2L+2, 2i\rho)$ is the confluent hypergeometric function of the first kind, which is $M \to 1$ for $\rho \to 0$. Here C_L is called a Coulomb constant:

$$C_L(\eta) = \frac{2^Le^{-\pi\eta/2}|\Gamma(L+1+i\eta)|}{\Gamma(2L+2)}. \tag{55}$$

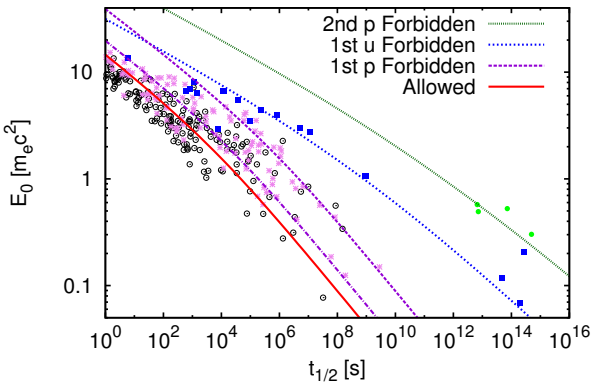

Figure 10: Energy and half-life of beta unstable r-process nuclides. Open circles, closes, filled squares, and filled circles are allowed, first parity forbidden, first unique forbidden, and second parity forbidden transitions respectively. Here the data points are taken from Evaluated Nuclear Data File ENDF/B-VII.1 library (**?**). Each curve depicts the theoretical expectation with a constant nuclear matrix element of each type of transitions: the allowed (red solid), the first parity forbidden (magenta dashed and dot-dashed), the first unique forbidden (blue dotted), and the second parity forbidden (green). Here we adopt $|\mathcal{M}_N|^2 = 0.05$ and $\langle Z \rangle = 50$ for all analytic models but $|\mathcal{M}_N|^2 = 0.01$ for the first unique transition.

Using these functions, we can see the wave function ψ has a finite amplitude at $r \sim 0$ when $l = 0$. For our case, the amplitude of the wave function at the origin is

$$\frac{|\psi(\eta;0)|^2}{|\psi(\eta=0;0)|^2} = |C_0(-\eta)|^2, \tag{56}$$

$$= \frac{e^{+\pi\eta}|\Gamma(1-i\eta)|^2}{\Gamma(2)^2}, \tag{57}$$

$$= \frac{2\pi\eta}{1-e^{-2\pi\eta}}, \tag{58}$$

where we have used $\Gamma(1+iy)\Gamma(1-iy) = |\Gamma(1+iy)|^2 = \pi y/\sinh \pi y$.

5.3 γ-ray heating

Beta decay often leads to a daughter nucleus in an excited state. The excited nucleus immediately decays to the ground state and emits γ-rays. Unfortunately, unlike β decay, we cannot predict the energy spectrum of γ-rays without considering the structure of nuclei. The energy generation rate in γ-rays follows the beta decay heating rate and the typical energy of γ-rays is about 1 MeV (see figure 11).

5.4 Other types of decays

Alpha decay:

Spontaneous fission: Heavy nuclei can be split into two fragments. This process is called fission and releases a huge amount of energy per decay. The released energy can be estimated as follows. Imagine a uranium nucleus, of which the total number of nucleons is ~ 240 and the binding energy per nucleon is 7.6 MeV (see figure 1), is split into two nuclei of mass number ~ 120. The binding energy per nucleon of such nuclei is ~ 8.5 MeV. Therefore, the total energy released in a fission process should be approximately

$$240(8.5 - 7.6) = 220\,\mathrm{MeV}. \tag{59}$$

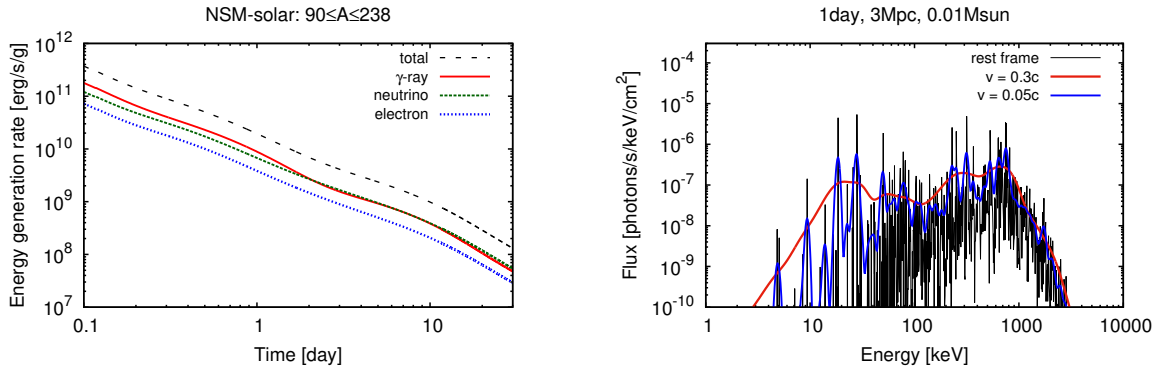

Figure 11: The energy production rate of different decay products (*left*). The γ-ray spectrum of r-process elements at 1 day after the nucleosynthesis (*right*).

Thus, the energy generation by fission is roughly 200 times more efficient compared to beta decay. Furthermore, as we will see in the next section, the thermalization efficiency of fission fragments is much more efficient. So if the ejecta contains small amounts of nuclei unstable against spontaneous fission with half-lives of the relevant time, they contribute the heating rate, in particular, at the later times. However, we have a little knowledge about the superheavy nuclei (heavier than uranium), which may be unstable against spontaneous fission. Their half-lives are quite uncertain and depends sensitively on the nuclear model (note that small uncertainties in the estimates of nuclear potential turns to a huge uncertainties in the half-life because it is in a exponential factor). In addition, they may decay from an excited state resulted from beta decay (beta-delayed fission). This effect likely reduces the abundance of superheavy nuclei that survive until the relevant timescale of kilonovae.

6 Thermalization efficiency

6.1 γ-ray thermalization

6.1.1 Compton Scattering

Consider the scattering process of radiation from free electrons (Compton scattering). In the frame where the electron is at rest initially, we can write the initial and final four momenta of the photon are $P_{\gamma,i} = (h\nu/c)(1, \vec{n}_i)$ and $P_{\gamma,f} = (h\nu_2/c)(1, \vec{n}_f)$ and the initial and final four momenta of the electron are $P_{e,i} = (m_e c, 0)$ and $P_{\gamma,f} = (E/c, \vec{p})$. The energy and momentum conservation leads to

$$h\nu_1 = \frac{h\nu}{1 + \frac{h\nu}{m_e c^2}(1 - \cos\theta)}, \tag{60}$$

where $\cos\theta = \vec{n}_{\gamma,i} \cdot \vec{n}_{\gamma,f}$. This can be rewritten as

$$\lambda_1 - \lambda = \lambda_c(1 - \cos\theta), \tag{61}$$

where λ_c is the Compton wavelength:

$$\lambda_c = \frac{h}{m_e c} = 0.02426 \mathring{A}. \tag{62}$$

The wavelength changes by the order of λ_c upon scattering. In the low energy limit, $\lambda \gg \lambda_c$, the scattering process is elastic. In the high energy cases, $h\nu > 10$ MeV, on the contrary, most of the photon energy can be transferred to the electron.

The Compton scattering cross section per electron is given by (the Klein-Nishina formula)

$$\sigma_{\rm Com} = \frac{3}{4}\sigma_T \left[\frac{1+x}{x^3} \left(\frac{2x(1+x)}{1+2x} - \ln(1+2x) \right) + \frac{1}{2x}\ln(1+2x) - \frac{1+3x}{(1+2x)^2} \right], \tag{63}$$

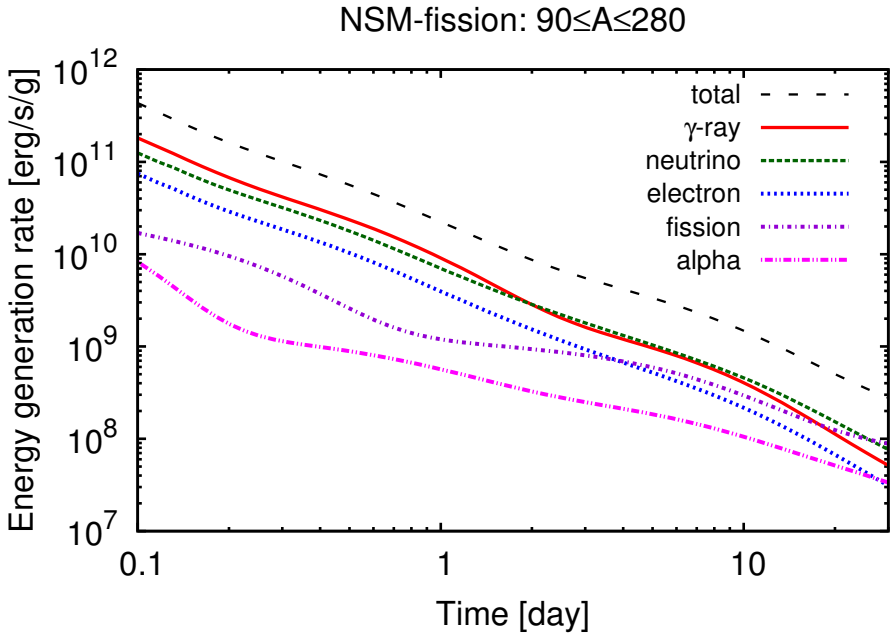

Figure 12: The energy production rate of different decay products including α decay and spontaneous fission.

where $\sigma_T = 8\pi e^2/3m_e c^2$ and $x = h\nu/m_e c^2$.

$$\sigma_{\rm Com} \approx \sigma_T \left[1 - 2x + \frac{26x^2}{5} + \mathcal{O}(x^3)\right], \qquad (x \ll 1), \tag{64}$$

whereas for the extreme relativistic regime we have

$$\sigma_{\rm Com} = \frac{3}{4}\sigma_T x^{-1}\left[\ln 2x + \frac{1}{2}\right] \qquad (x \gg 1), \tag{65}$$

One can see that the formula recovers the Thomson scattering cross section in the non-relativistic limit and the Compton scattering cross section decreases with photon energy as $\ln x/x$. This is the well known Klein-Nishina suppression of the cross section in the relativistic limit.

6.1.2 Photoelectric absorption

Photons are efficiently absorbed by atoms when the photon energy is comparable to the ionization energy of the atoms ($\lesssim 100$ keV for r-process elements). For energies greater than the K-shell ionization energy, E_K, (K-shell is the most bound electron orbit), the absorption process is dominated by the K-shell ionization:

$$\sigma_{\rm ph,K} = 4\pi\sqrt{2}Z^5\alpha^4\sigma_T\left(\frac{m_e c^2}{h\nu}\right)^{7/2}\Theta(h\nu - E_K), \tag{66}$$

where $\Theta(x)$ is the Heaviside function. For heavy r-process elements, the photoelectric absorption dominates over the other process below ~ 0.5 MeV.

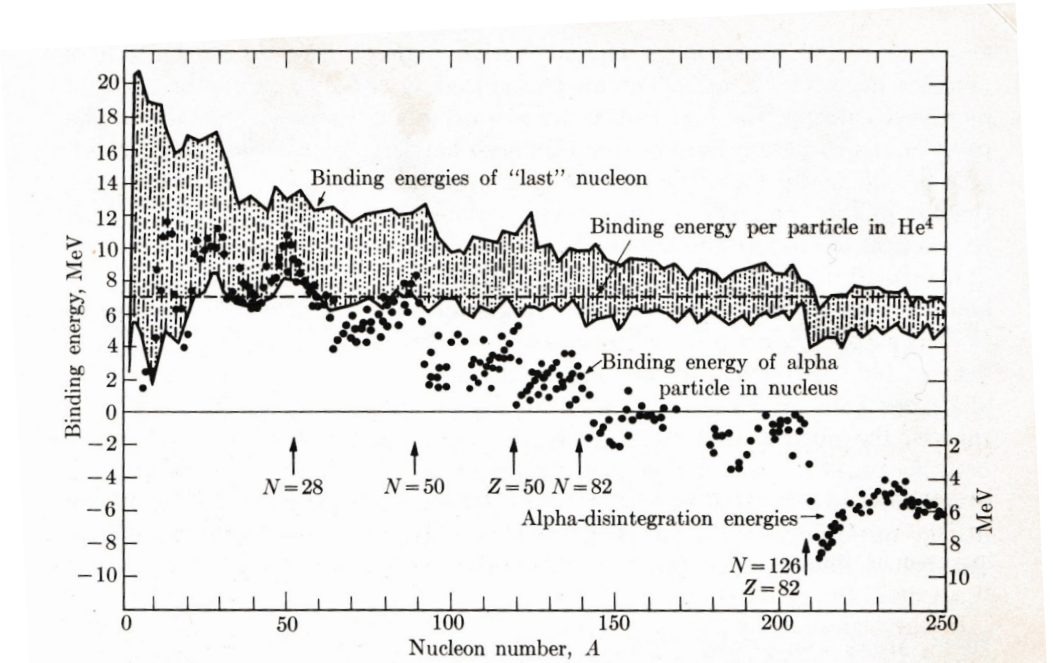

Fig. 10–1. Minimum and maximum binding energy for "last" nucleon and binding energies of "last" alpha particle for beta-stable nuclei.

Figure 13: Alpha decay.

6.1.3 Pair production (Bethe-Heitler process)

At energies of $> 2m_ec^2(1.022, \mathrm{MeV})$, photons can produce electron-positron pairs as result of the interaction with the nuclear electric field. The cross section of the pair production is given by

$$\sigma_{\mathrm{pair}} = Z^2\alpha^2 \left(\frac{e^2}{m_ec^2}\right)^2 \left(\frac{28}{9}\ln\frac{2h\nu}{m_ec^2} - \frac{218}{27}\right). \tag{67}$$

This expression is valid for $2m_ec^2 \ll h\nu \ll \frac{m_ec^2}{\alpha Z^{1/3}}$. As one can see, the cross section is logarithmically increased with photon energy and is strongly enhanced with the proton number Z. For r-process elements, the pair production is the dominant process stopping γ-rays at photons energies greater than ~ 5 MeV.

6.2 Thermalization of charged particles

6.2.1 Ionization loss

Consider that a charged particle of m and Z moving with a velocity of v passes by an electron in an atom at rest with an impact parameter b (Fig. 16). Here we assume that the velocity is so great that in most cases (b is sufficiently large) the electron has not appreciably changed its position before the particle has passed by. The electron does get a net impulse given be

$$p = \int_{-\infty}^{\infty} F\sin\theta dt, \tag{68}$$

where the force F is the Coulomb force Ze^2/r^2 and the distance can be expressed as $r = b/\sin\theta$. As the Coulomb force decreases with radius as $\propto r^{-2}$, the amount of impulse is dominated around the closest approach $r \approx b$, of which the duration is $\Delta t \approx b/v$. Therefore, the total impulse is roughly

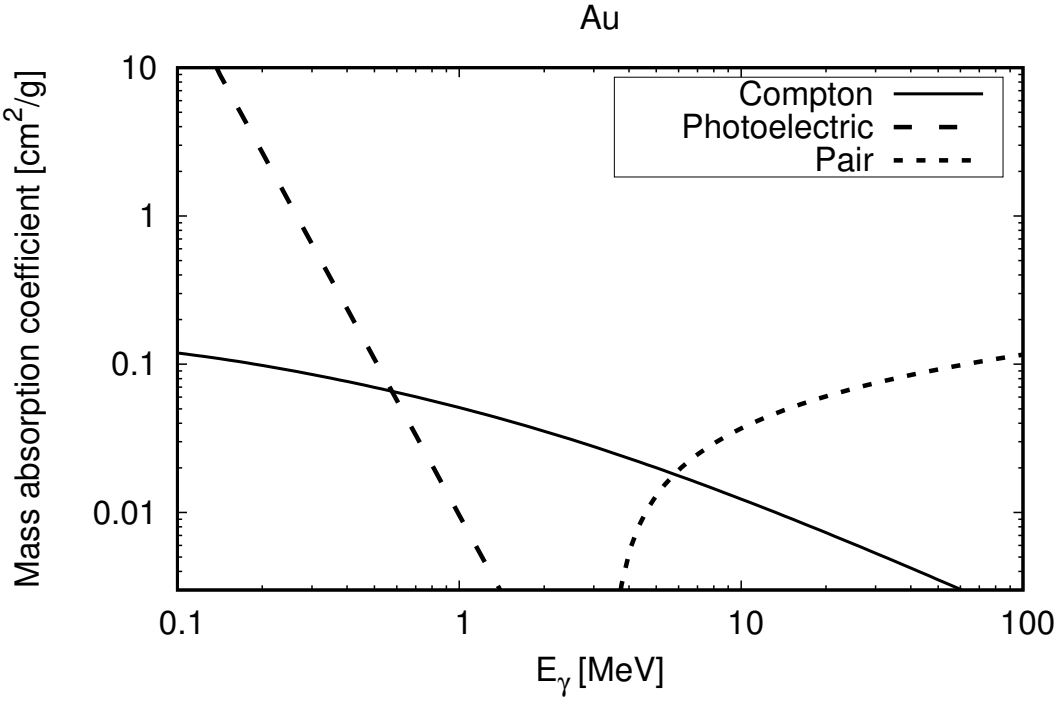

Figure 14: Mass absorption coefficient Au for the Compton scattering, photoelectric absorption, and pair production.

$p \approx Ze^2/bv$. Of course, we can perform the integration of equation (68) exactly. There is a relation between t and θ as $dt = bd\theta/v\sin^2\theta$. We find the momentum of the electron after the particle has passed:

$$p = \int_0^\pi \frac{Ze^2 \sin\theta d\theta}{bv} = \frac{2Ze^2}{bv}. \tag{69}$$

Assuming that the velocity of the electron is sufficiently low so that we can use classical formulas, we find the kinetic energy of the electron as a function of impact parameter:

$$T_e = \frac{p^2}{2m_e} = \frac{2Z^2e^4}{b^2 m_e v^2}. \tag{70}$$

The ionization cross section can be obtained by setting $T_e = I_{nl} = Z_T^2 E_0/2$, where Z_T is the target's effective nuclear charge and $E_0 = m_e v_0^2 = 2Ry$, and $v_0 = e^2/\hbar$:

$$\sigma_i^{\rm Bohr} = \frac{2\pi Z^2 e^4}{m_e v^2 I_{nl}} \tag{71}$$

$$= 2\pi Z^2 a_0^2 \frac{v_0^2 E_0}{v^2 I_{nl}}, \tag{72}$$

where $a_0 = \hbar^2/m_e e^2 = \hbar/v_0 m_e$. Note that we have assumed the velocity of the target electron is zero. However, the bound electron has a finite orbital velocity, which helps to eject the electron via collision.

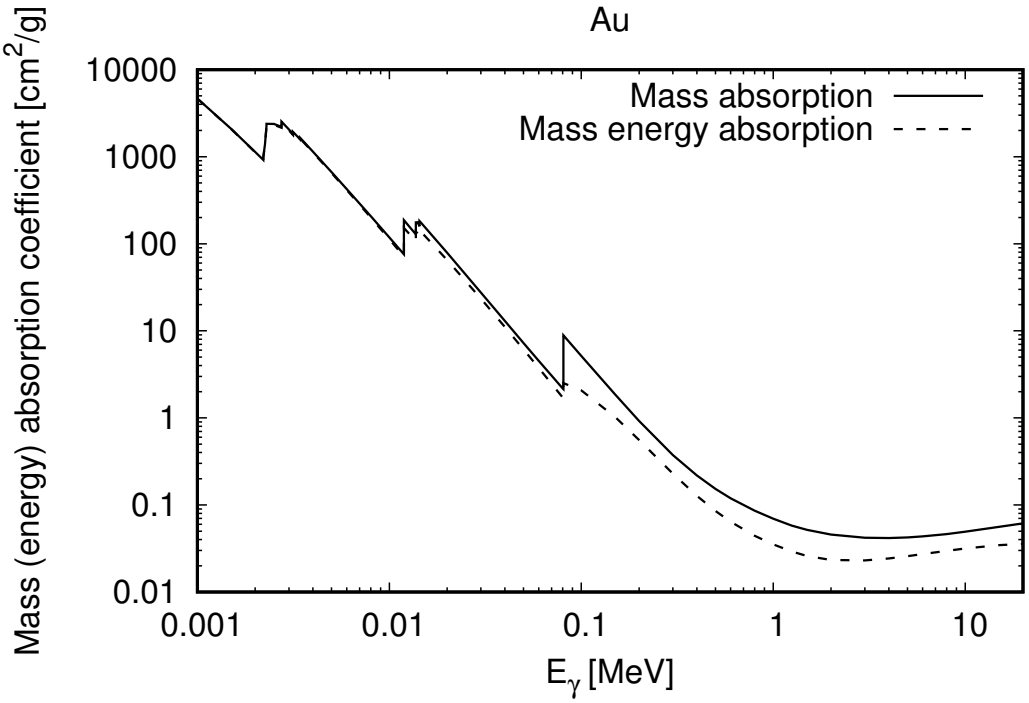

Figure 15: Mass absorption coefficient and mass energy coefficient of Au.

The differential cross section is

$$\frac{d\sigma}{dW} = 2\pi Z^2 a_0^2 \frac{v_0^2 E_0}{v^2 W^2} \tag{73}$$

Bethe calculated the ionization cross section with the Born approximation and found for $v \gg v_{nl}$

$$\sigma_i^{\text{Bethe}} = \sigma_i^{\text{Bohr}} \left(0.566 \ln \left(\frac{v}{v_{nl}} \right) + 1.261 \right). \tag{74}$$

The stopping cross section, which has a dimension of area times energy, is defined as

$$\sigma_e = \int \Delta T dA, \tag{75}$$

where ΔT is the loss of kinetic energy sustained by the particle when moving through the area dA. Ordinarily, a cross section is a measure of the probability of removing a particle from the primary beam. Here instead, we are interested in the process that the particle is only slowed down. Using equation (70), we get

$$\sigma_e \int_{b_1}^{b_2} T_e 2\pi b db = \frac{4\pi Z^2 e^4}{m_e v^2} \ln \frac{b_2}{b_1}, \tag{76}$$

where $b_1 \approx h/2m_e v$ is determined by the uncertainty principle and $b_2 \approx v/\nu$, where ν is an average of the frequencies of oscillations of the electrons in the atom.

$$\sigma_e = \frac{4\pi Z^2 e^4}{m_e v^2} \ln \frac{2m_e v^2}{\langle I \rangle}, \tag{77}$$

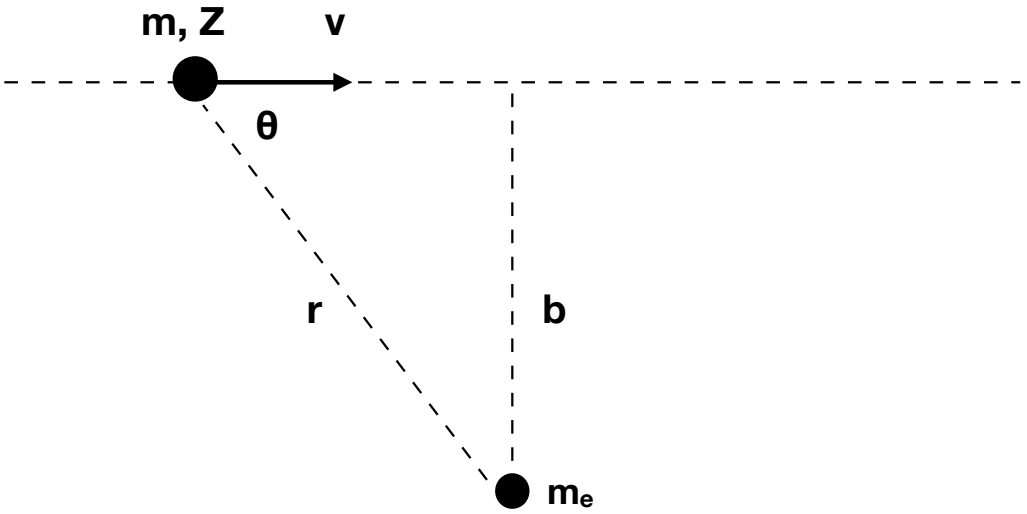

Figure 16: The collision of a charged particle with an electron.

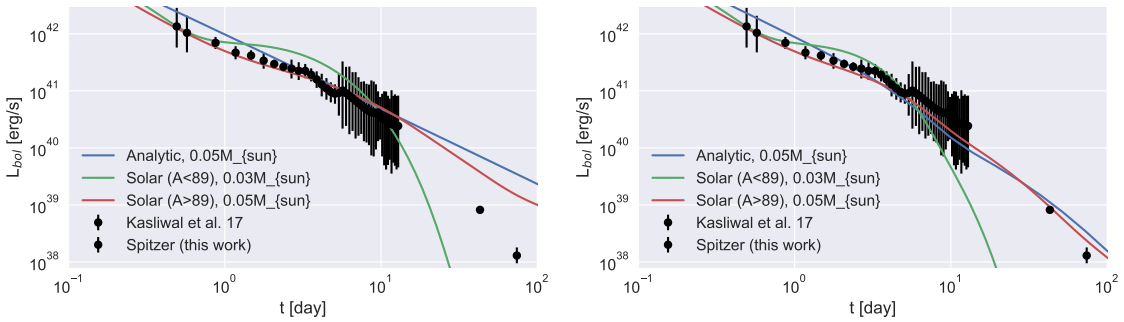

Figure 17: The bolometric light curve of the kilonova GW170817 and beta-decay heating rate. *Left:* the total heating rates without taking into account for the thermalization efficiency and *Right:* the ones with the thermalization efficiency.

where $\langle I \rangle = h\langle \nu_{nl} \rangle$ is the an average excitation energy or binding energy for the electrons in the atoms of the stopping medium.

The formula valid for in the relativistic regime is given by

$$\sigma_e = \frac{2\pi Z_{\rm ion} e^4}{m_e v^2} \left[\ln\left(\frac{m_e v^2 T}{2\langle I \rangle^2 (1-\beta^2)} \right) - (2\sqrt{1-\beta^2} - 1 + \beta^2) \ln 2 + 1 - \beta^2 + \frac{1}{8}(1-\sqrt{1-\beta^2})^2 \right]. \quad (78)$$

6.2.2 Bremsstrahlung

6.3 Heavy particles

The stopping cross section for a heavy particle of $M \gg m_e$ and an electric charge Z moving in a medium composed of neutral ions with an atomic number $Z_{\rm ion}$ at a velocity v is

$$\sigma_{\rm st}(v) = \frac{4\pi Z^2 Z_{\rm ion} e^4}{m_e v^2} \left[\ln\left(\frac{2 m_e v^2}{\langle I \rangle} \right) - \ln\left(1-\beta^2\right) - \beta^2 \right]. \quad (79)$$

Comparing equation (79) to equation (78), one can see that the stopping cross section of heavy particles is much greater than that of electrons for a same kinetic energy.

7 GW170817

References

Colgate S. A., White R. H., 1966, ApJ, 143, 626

Fermi E., 1934, Z. Phys., 88, 161

Goriely S., Bauswein A., Janka H.-T., 2011, ApJL, 738, L32

Hotokezaka K., Wanajo S., Tanaka M., Bamba A., Terada Y., Piran T., 2016, MNRAS, 459, 35

Konopinski E. J., 1966, The Theory of Beta Radioactivity. Oxford University Press

Korobkin O., Rosswog S., Arcones A., Winteler C., 2012, MNRAS, 426, 1940

Lippuner J., Roberts L. F., 2015, ApJ, 815, 82

Metzger B. D., Martínez-Pinedo G., Darbha S., Quataert E., Arcones A., Kasen D., Thomas R., Nugent P., Panov I. V., Zinner N. T., 2010, MNRAS, 406, 2650

Roberts L. F., Kasen D., Lee W. H., Ramirez-Ruiz E., 2011, ApJL, 736, L21

Wanajo S., Sekiguchi Y., Nishimura N., Kiuchi K., Kyutoku K., Shibata M., 2014, ApJL, 789, L39